Towards a practical solution for removing inorganic mercury from drinking water using gold nanoparticles

K.P. Lisha, Anshup and T. Pradeep*

DST Unit on Nanoscience (DST UNS)
Department of Chemistry and Sophisticated Analytical Instrument Facility, Indian Institute of Technology Madras, Chennai 600 036, India

* Corresponding author: Fax: + 91-44 2257-0545
E-mail: pradeep@iitm.ac.in

Abstract

We describe an innovative approach based on alloying of metals to remove metal ions from drinking water. A novel adsorbent, gold nanoparticle supported on alumina, was developed for the removal of inorganic mercury from water. The observed adsorption capacity for mercury is 4.065 gm per gm of gold nanoparticles, which is ~10 times higher metal adsorption capacity than previously reported adsorbents. Gold nanoparticle has been supported on alumina, at a capacity of 738 mg/kg alumina, for use in practical applications. Batch and column studies were done for adsorption analysis and a practical filter has been developed. The interaction between gold and mercury was studied using UV-vis, TEM, SEM, EDAX and XRD. The chemistry of metal alloying can be utilized for sequestration of mercury from drinking water. Established separation techniques for recovery of metals from the alloy can be utilized, making this a complete solution for drinking water applications.

Keywords: Adsorption; Gold nanoparticles; Drinking water purification; Sodium borohydride; Rhodamine 6G; Alumina; Amalgam

Introduction

Mercury is a highly volatile and highly toxic heavy metal present in the environment. Inorganic mercury in water is mainly seen in the +2 oxidation state. Mercury is released into the atmosphere through a variety of natural and anthropogenic sources [1]. Natural sources include volcanic eruptions, mercury rich soil and forest fires. Mobilization of mercury from fossil fuels, incinerators, chlor-alkali industries, gold mining, processing and refining of mercury ores are few of the major anthropogenic sources [2]. Once released into the environment, it can undergo complex physical and chemical transformations. Released mercury vapour gets converted into soluble form and gets deposited in soil and water by rain. Due to microbial action, inorganic mercury gets converted into methyl mercury and enters the food chain of predatory species. Low dose mercury exposure can affect various organ systems of adults and children. In adults it can lead to memory loss, Alzheimer's like dementia, decreased rate of fertility, birth of abnormal offspring, etc. In children the effects include autism, late walking and deficit in memory and language [3]. In the world the first mercury pollution reported in Minamata City located on the Yatsushiro Sea coast in Kumamoto Prefecture of Japan in 1956, was due to the poisoning of the central nervous system caused by methyl mercury which accumulated in fish and shellfish, as a result of mercury released into Minamata Bay [4, 5]. Due to the severe effects of mercury on mankind, World Health Organization (WHO) has set the limit for mercury in drinking water to be 0.001 mg/L [6]. Due to its diverse properties, mercury is still used in different areas like electrical industry, dentistry, mining, catalysis, etc. [7]. Studies show that mercury pollution is a threat to human beings in the developing countries even now [8]. Reports show that the concentrations of mercury in ground water in a few industrial areas of India are more than the standards set by WHO and the Bureau of Indian Standards [6, 9]. According to this, the concentration of mercury in a few industrial areas in the states of Gujarat, West Bengal, Orissa, Haryana and Andhra Pradesh are ten or twenty times higher than the maximum permissible limit. These alarming levels are mainly due to the discharge of mercury bearing effluents having concentrations ranging from 0.058 to 0.268 mg/L. It is against the permissible limit of mercury (0.01 mg/L) set by Indian standards for effluent discharge [8].

Different technologies like adsorption, ion exchange, amalgamation and chemical precipitation are available for the removal of mercury from contaminated water [10-20]. Nanomaterials are highly promising in the water purification process due to their unique properties like higher surface area per unit volume, ease with which they can be anchored onto solid matrices and the ability to functionalize with different functional groups to enhance their affinity towards target molecules. There are many reports on the use of nanoparticles for water purification [21, 22]. The use of gold

nanoparticles in water purification is an emerging field. Our group has investigated the use of gold nanoparticles for the detection and removal of various organochlorine compounds (e.g. pesticides such as chlorpyrifos and halocarbons such as carbon tetrachloride) from drinking water [23-25]. Gold nanoparticles supported on silica and titania and bimetallic Au-Pd have been investigated for environmental remediation of various organic compounds [26-32]. There are reports on the removal of mercury from aqueous solution using nanoparticles of alumina and thiol functionalized superparamagnetic Fe_3O_4 [33, 34]. An alumina refinery aqueous stream was treated with nanoparticle systems like gold impregnated silica and silver impregnated silica for the removal of mercury [35].

In this paper we describe the complete removal of mercury from water using gold nanoparticles supported on alumina. Affinity of mercury to gold is well-known since ancient times. Nanomaterials, the product of contemporary science are well-known for their large surface area. We applied the amalgamation of these two for the effective removal of mercury from water. We have conducted batch and column experiments for finding the mercury removal capacity of supported gold nanoparticles. We have done various spectroscopic and microscopic examinations for understanding the interaction between gold and mercury. Mercury removal capacity of this material is very high and it can be applied for water purification economically.

Experimental section

Chemicals used

Tetrachloroauric acid trihydrate ($HAuCl_4.3H_2O$) was purchased from CDH India. Trisodium citrate and sodium borohydride ($NaBH_4$) were purchased from SRL India and Aldrich, respectively. A stock solution of 500 mg/L Hg(II) was prepared from $HgCl_2$ (Glaxo Laboratories Limited) and required concentrations were made by serial dilution. Rhodamine 6G was purchased from Fluka and azomethine-H-monosodium salt, monohydrate was from HiMedia Laboratories Pvt. Limited, India. Magnesium oxide was purchased from Thomas Baker and neutral activated alumina (140 mesh, 150 m^2/g) was from a local source and used as received. Triple distilled water was used throughout the experiment.

Instrumentation

UV-vis absorption spectra were performed on a Perkin-Elmer Lambda 25 spectrometer. Low mercury concentrations (<0.2 mg/L) in the solutions were detected by a Mercury Analyzer MA 5840. Mercury analyses in the concentration range of 0.2 to 2.0 mg/L were done using colourimetry. High resolution transmission electron microscopy (HRTEM) was carried out using a JEOL 3011, 300 kV instrument with a UHR polepiece. Scanning electron microscopic (SEM) images and energy dispersive analysis of X-ray (EDAX) studies were done in a FEI QUANTA-200 SEM. X-ray diffraction (XRD) data were collected with a Bruker AXS, D8 Discover, U.S.A., diffractometer using Cu-Kα radiation (λ=1.54 Å). The samples were scanned in the 2θ range of 10-90 degrees.

Synthesis of supported gold nanoparticles

Gold nanoparticles with an average diameter of 10-20 nm were synthesized by the reduction of $HAuCl_4.3H_2O$ with trisodium citrate [36]. Supported gold nanoparticles were prepared by the following procedure. 10 g of neutral activated alumina were soaked in 25 mL of gold nanoparticle suspension for 30 minutes. Once the supernatant became colourless, it was replaced with another fresh 25 mL suspension. This procedure was repeated until there was no colour change for the supernatant. After decanting the supernatant, gold nanoparticle-coated alumina were washed thoroughly with distilled water and dried under ambient condition. The intake of gold nanoparticle was about 738 mg per 1 kg alumina.

Uptake of mercury

The interaction between supported gold nanoparticles and Hg(II) ions was studied using a column set-up. 2 g of gold nanoparticle-coated alumina was taken in the column and 1.0 mg/L Hg(II) solution was passed through it at a flow rate of 5 mL/minute. 5 mL of the treated water was collected at an interval of 100 mL and analysed for residual mercury using UV-vis spectroscopy [37]. The experiment was continued till mercury was detected in the treated sample. A calibration graph was drawn using known concentrations and the absorbance at 570 nm due to the complex formed between tetraiodomercurate and rhodamine 6G.

For studying the interaction of supported gold nanoparticles with Hg(0), 1.0 mg/L Hg(II) was reduced with dilute aqueous $NaBH_4$ (10 times the mercury concentration) and allowed to stand for 1 h. Afterwards, the solution was passed through a column containing 2 g of gold nanoparticle-coated alumina. 5 mL of the treated water was collected at an interval of 100 mL. Before analysis, the sample collected was treated with concentrated HCl for the oxidation of Hg. The experiment was continued till mercury was detected in the sample. Same experiment was repeated with 2.0 mg/L Hg(II) also. In order to find the interaction of Hg(0) with alumina, the experiment was repeated with 2 g of alumina.

A study was done with 0.2 mg/L mercury for understanding the interaction of low concentrations of mercury with supported gold nanoparticles. 4 g of gold nanoparticle-coated alumina was taken in the column and mercury solution was passed at a rate of 5 mL/minute. 50 mL of the treated water was collected at an interval of 1 L. Mercury concentration in the sample was detected using a mercury analyzer at 253.7 nm.

Batch experiments were done for finding the interaction of supported gold nanoparticles with mercury. For the study, 1 g of gold nanoparticle-coated alumina was transferred to

$NaBH_4$ treated 500 mL of 1.5 mg/L Hg(II) and stirred continuously. 5 mL of the sample was collected at different time intervals and centrifuged, supernatant was collected for mercury measurement.

Characterisation of gold-mercury system

A solution phase experiment was done with the as prepared gold nanoparticles for understanding the interaction between gold nanoparticles and mercury. 2.5 mL of 2.0 mg/L Hg(II) was mixed with $NaBH_4$ and added to 2.5 mL gold nanoparticle suspension and UV-vis spectra were recorded. For understanding the changes in morphology, TEM analysis of the sample before and after mercury addition was done. The change in the morphology of gold nanoparticle was studied using SEM analysis of the mercury-treated gold nanoparticle solution. EDAX spectra and images were measured for finding the elemental composition and distribution in the nanoparticles after mercury addition. XRD analyses of the gold nanoparticles and mercury treated gold nanoparticles were carried out for understanding the structural changes.

Detection and removal of boron

For testing the presence of boron in the treated water, 10 mL of the sample was collected from the column outlet and analysed for boron by a simple procedure proposed by Lopez et al. [38]. In order to have a larger boron concentration in the treated water, a column study was done with 2.0 mg/L Hg(II) reduced with 20 times $NaBH_4$. Performance of magnesium oxide as a boron adsorbent was tested [39]. 250 mg of magnesium oxide was transferred to 50 mL of the polluted water and stirred continuously. The samples collected at different time intervals were centrifuged and the supernatant was analysed for boron.

Results and discussion

Uptake of mercury

Figure 1A is a schematic diagram of the down-flow column apparatus used for mercury removal studies. The column used was 1.5 cm in diameter and 30 cm in height. Inset of Figure 1A shows a photograph of the adsorbent, gold nanoparticle-supported alumina. The adsorbent was packed in the column and the flow rate through the column was controlled by a peristaltic pump. Figure 1B shows the UV-vis absorption spectra for the elution of 1.0 mg/L Hg(II) passed through the column containing 2 g of gold nanoparticle-coated alumina. Traces 'a-d' are the absorption spectra after flowing 0.10, 0.20, 0.30 and 0.40 L, respectively. The absorption spectra for these samples are the same as that of rhodamine 6G. It is a clear indication of the absence of mercury in the treated water. Trace 'e' is for 0.50 L and it showed the absorbance at 570 nm. The intensity of the peak at 570 nm indicated Hg(II) concentration of 0.31 mg/L. Trace 'f' is for 0.60 L and the concentration of Hg(II) is 0.83 mg/L. The loading of Hg(II) on gold nanoparticle-coated alumina is 200 mg/kg, in terms of gold it is 200 mg of Hg(II) per 738 mg gold. This uptake capacity is relatively low. It may be due to the poor physical interaction between gold nanoparticle and Hg(II) ions. The inset of Figure 1B shows the concentration versus bed volume.

Figure 1

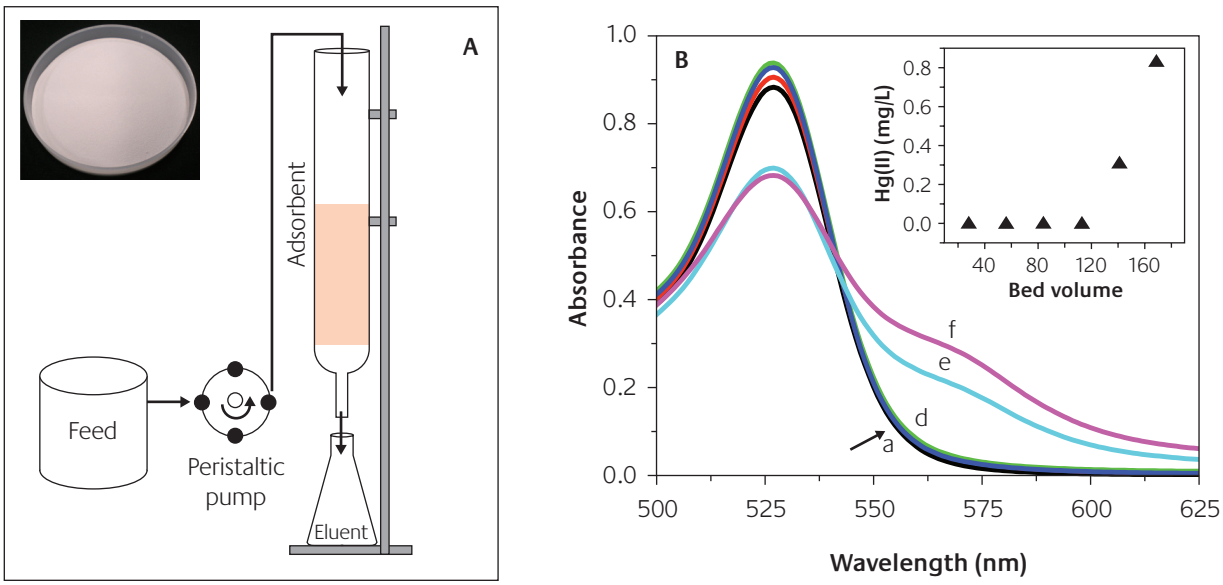

(A) Schematic representation of the down-flow column apparatus. Inset is a photograph of gold nanoparticle-supported alumina. (B) UV-vis absorption spectra of the solution as 1.0 mg/L Hg(II) was flown through the column. Traces 'a-d' are the absorption spectra corresponding to the passage of 0.10, 0.20, 0.30 and 0.40 L, respectively. Trace 'e' is for 0.5 L and trace 'f' is for 0.6 L, respectively. Inset is the plot of concentration versus bed volume

Figure 2

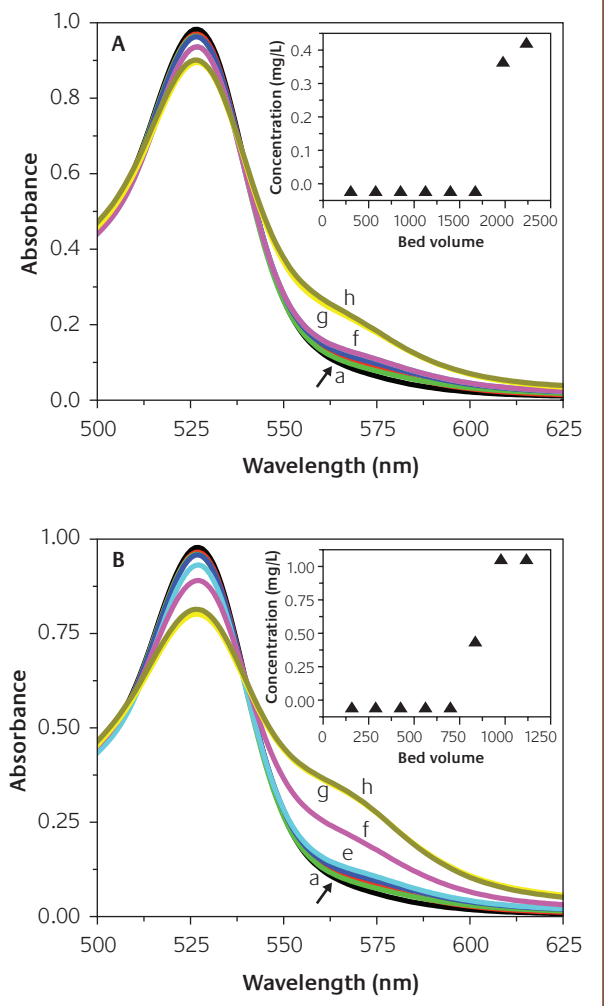

(A) UV-vis absorption spectra of the solution as 1.0 mg/L Hg(0) was passed through the column. Traces 'a-f' are the absorption spectra for the first 6 L, at an interval of 1 L. Trace 'g' and trace 'h' are the absorption spectra for 7 and 8 L, respectively. (B) Corresponding data for 2.0 mg/L Hg(0). Traces 'a-e' are the absorption spectra of 0.5, 1.0, 1.5, 2.0 and 2.5 L, respectively. Traces f, g, h are for 3.0, 3.5, 4.0 L, respectively. Insets are plots of concentration versus bed volume for each case

To improve the mercury uptake by supported nanoparticles, we studied the interaction of Hg(0) with gold nanoparticles after reducing Hg(II) with $NaBH_4$. Figure 2A shows the UV-vis absorption spectra for the elution of 1 mg/L Hg(0) through a column containing 2 g of gold nanoparticle-supported alumina as the adsorbent. Traces 'a-f' are the absorption spectra for the first 6 L. There is no absorbance at 570 nm in these spectra indicating the absence of mercury in the treated samples. Trace 'g' and trace 'h' are the absorption spectra for 7 and 8 L, respectively. The absorbance at 570 nm in these spectra is due to mercury and the concentration is 0.356 and 0.419 mg/L, respectively. The loading capacity of Hg(0) is 4.065 gm per gm of gold nanoparticle. The loading capacity of Hg(0) expressed in terms of gold nanoparticle-coated alumina is 3000 mg/kg.

The extremely high uptake capacity on gold nanoparticle surface may be due to the gold mercury amalgam and the formation of amorphous mercury layer formation over gold nanoparticle surface. The inset of Figure 2A is the plot of mercury concentration versus the bed volume.

Adsorption study with 2.0 mg/L Hg(0) was tried on 2.0 g of gold nanoparticle-supported alumina. Figure 2B shows the UV-vis absorption spectra corresponding to the treated water. Traces 'a-e' are the absorption spectra of 0.5, 1.0, 1.5, 2.0 and 2.5 L, respectively. There is no 570 nm absorbance in these spectra. Traces f, g, h are for 3.0, 3.5, 4L, respectively

Figure 3

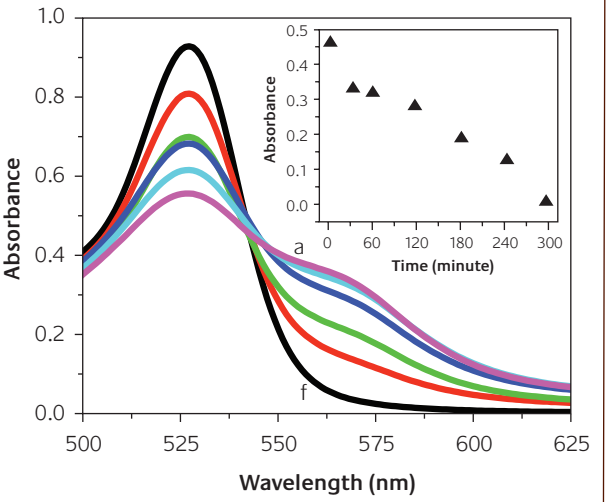

UV-vis absorption spectra of samples collected at different time intervals in a batch reaction using 1.5 mg/L Hg(0). Trace 'a' shows the absorption spectrum of the supernatant collected after 30 minutes. Traces 'b-f' are the absorption spectra collected at 1, 2, 3, 4 and 5 h, respectively. Inset is the plot of absorbance versus time

Figure 4

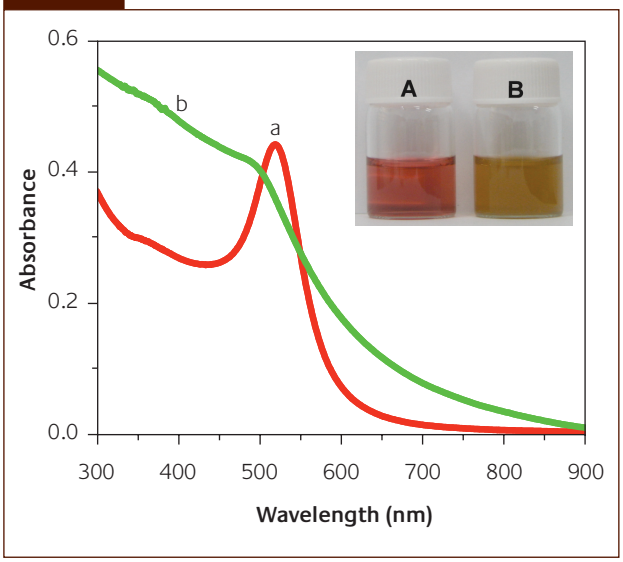

The UV-vis absorption spectra of gold nanoparticles (a) before and (b) after mercury treatment. Inset is the photograph of gold nanoparticles and mercury treated gold nanoparticles

and the absorbance at 570 nm is very clear. Inset of Figure 2B is the plot of mercury concentration versus bed volume.

The treated water collected after passing 10 L of 0.2 mg/L Hg(0) through 4 g gold nanoparticle-supported alumina, in a similar column, showed complete removal.

The interaction between Hg(0) and the pure substrate (alumina) was also studied. By passing 0.25 L of 1.0 mg/L Hg(0), alumina (2 g) got exhausted.

Figure 3 shows the absorption spectra collected at different time intervals in a batch reaction of gold nanoparticle-supported alumina with 1.5 mg/L Hg(0). Trace 'a' is the absorption spectrum of the supernatant collected after 30 minutes. It shows intense absorption at 570 nm. Traces 'b-f' are the absorption spectra collected at 1, 2, 3, 4 and 5 h, respectively. Inset in the figure shows a plot of absorbance versus time. It shows a gradual reduction in the absorption at 570 nm and by the fifth hour, complete disappearance occurs. It may be due to the slow adsorption of mercury on gold nanoparticles under vigorous stirring.

Characterisation of gold-mercury system

The nature of Hg(0) interaction with gold nanoparticle was investigated with a variety of tools. UV-vis spectroscopy was used to characterise the gold colloid before and after mercury treatment. Figure 4 shows the UV-vis absorption spectra of gold nanoparticles before and after mercury treatment.

Figure 5

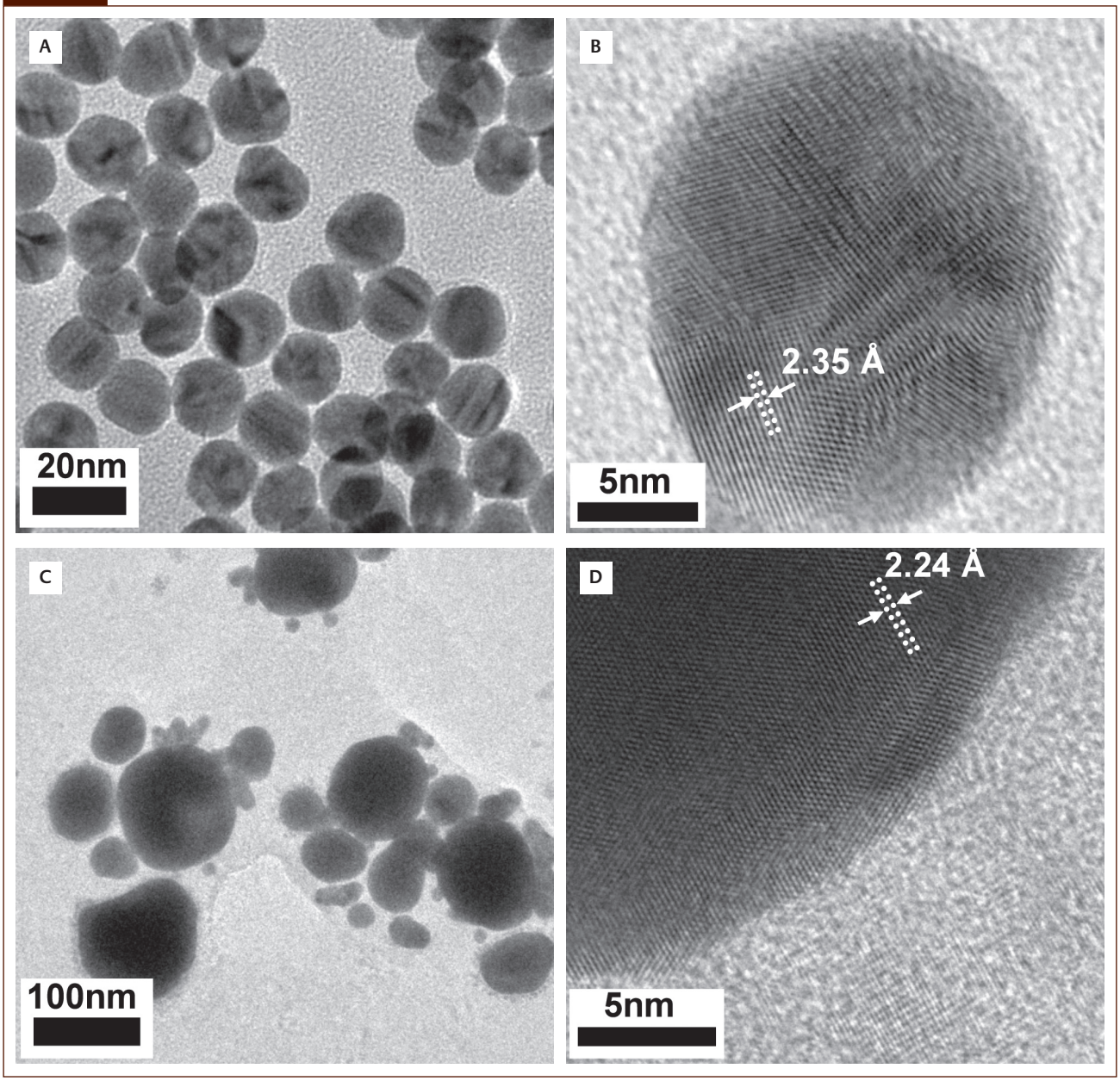

TEM images of gold nanoparticles before and after mercury treatment. (A) Large area image of gold nanoparticles before the reaction. (B) The corresponding lattice resolved image of a single nanoparticle. (C) Large area image of mercury treated gold nanoparticles. (D) The corresponding lattice resolved image of a single nanoparticle

Figure 6

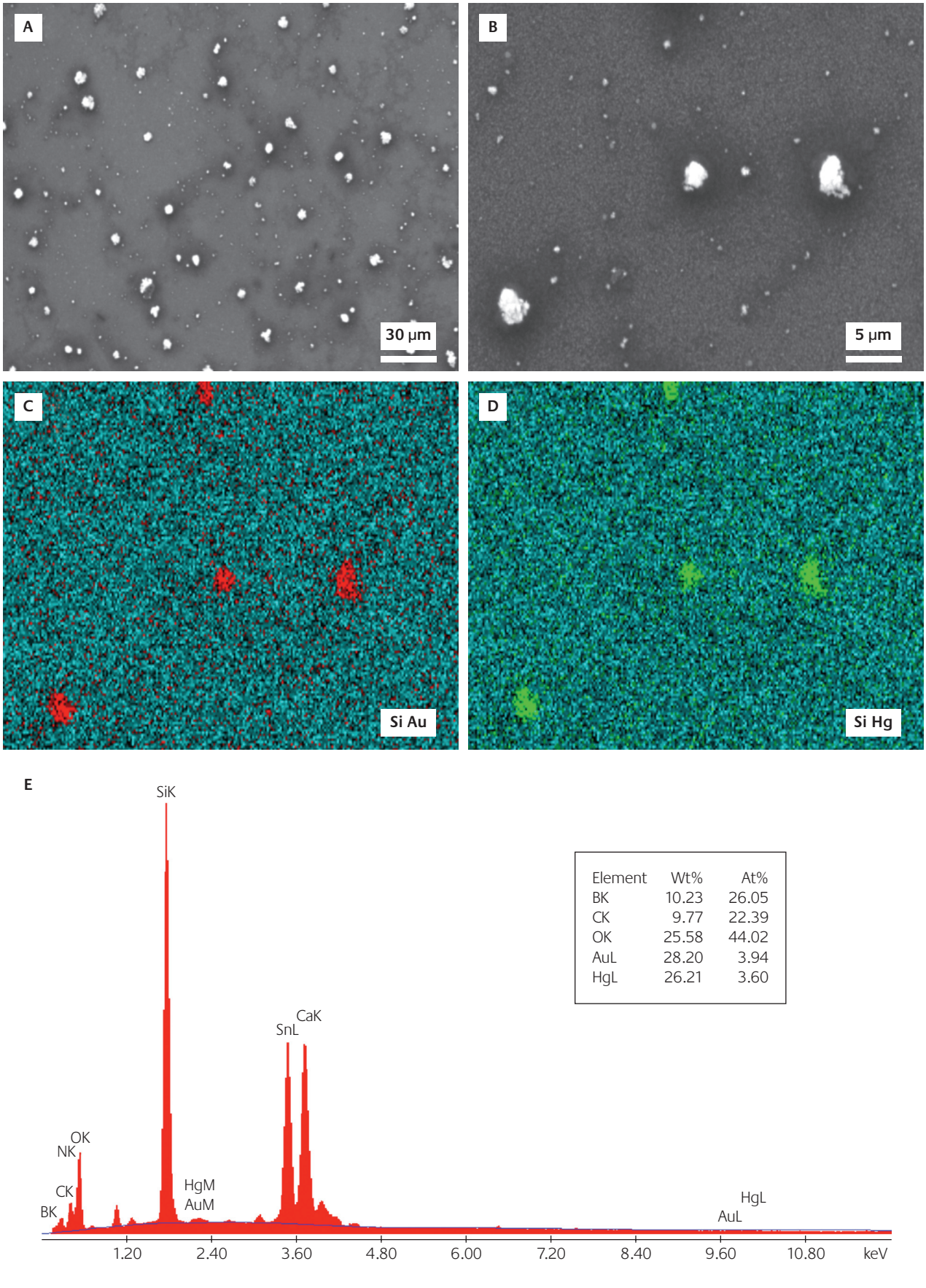

SEM images of mercury treated gold nanoparticles. (A) Large area image, (B) magnified image of few particles, (C) elemental map of Au, (D) elemental map of Hg and (E) EDAX spectrum of mercury treated gold nanoparticles. Inset is the composition table

Trace 'a' is the absorption spectrum of the as prepared gold nanoparticles and it exhibits a characteristic absorption at 520 nm due to the surface plasmon resonance. Trace 'b' is the absorption spectrum of the $NaBH_4$ treated Hg(II) solution in gold colloid showing a maximum absorbance at 490 nm. Although the peak shift is small, the peak shape has got modified significantly. The shift in the peak position is an indication of Au/Hg particles with different morphology [40]. Inset shows the photographs of the as prepared gold nanoparticles (A) and mercury treated gold nanoparticles (B). The wine red colour of the gold nanoparticle solution changes into brownish orange after the addition of mercury solution.

Figure 5A shows the large area TEM image of the as prepared gold nanoparticles. The nanoparticles are spherical in shape and are uniformly distributed as typical of citrate synthesis. Their size distribution is remarkably narrow and is within 16±2 nm. Lattice resolved image of an individual gold nanoparticle is given in Figure 5B. A lattice spacing of 2.35 Å is seen, which corresponds to the (111) plane of gold. Multiple twinning is evident. Figure 5C shows a large area image of mercury treated gold nanoparticles. The nanoparticles are of varying sizes and there is a large distribution. The image shows several larger particles being surrounded by smaller particles. It appears that the larger particles are undergoing Ostwald ripening. Figure 5D shows the lattice resolved image of an individual mercury treated gold nanoparticle. The nanoparticle exhibits a lattice spacing of 2.24 Å, which corresponds to the (101) plane of Au_3Hg alloy. No core-shell morphology is seen and it appears that the product formed is a continuous phase. It is clear that the ionic shell formed by the protecting group is disturbed due to Hg uptake, which contributes to the fusion of the particles.

SEM images of mercury treated gold nanoparticles were taken for understanding the morphology. Figure 6A and Figure 6B are the large area SEM images of mercury treated gold nanoparticles. The image shows that some particles are very large in size and are distributed randomly. The morphology of the particles is different and they possess a thin surface layer which may be due to the presence of mercury. Elemental maps of Au and Hg overlaid on Si (from glass substrate) are shown in Figures 6C and 6D, respectively. From the elemental analysis it is clear that gold and mercury are equally distributed in the particles. The uniform distribution of gold and mercury may be due to the amalgam formation. This is supported by the TEM measurements as well. Figure 6E shows the EDAX spectrum of the particles in Figure 6B. Inset gives the composition. From the figure it is clear that the nanoparticles formed are gold-mercury bimetallic alloys and their distribution is nearly uniform. Si and Sn are due to the substrate used.

XRD analysis shows the existence of Hg and Au_3Hg in the treated sample. The XRD pattern of gold nanoparticles which exhibits all the peaks expected for gold [41] at 38.17°, 44.38°, 64.57°, 77.56° and 81.72° in 2θ. The peaks correspond to gold (111), (200), (220), (311) and (222) planes, respectively. The XRD pattern of mercury treated gold nanoparticles show peaks at 35.62°, 37.47°, 40.44°, 52.59°, 63.74°, 69.64°, 76.51°, 78.37° and 79.94° in 2θ. The peaks correspond to (100), (002), (101), (102), (110), (103), (112), (201) and (004) planes of Au_3Hg [42]. The peaks observed at 31.64°, 39.01°, 66.09° and 83.81° in 2θ correspond to the (110), (101), (220) and (202) planes of Hg-tetragonal [43]. The inconsistency between the EDAX and XRD data appear to be because XRD samples a much larger area.

From the XRD pattern and HRTEM analyses of gold nanoparticles and mercury treated gold nanoparticles the mechanism of mercury removal by gold nanoparticles can be attributed to amalgamation between mercury and gold. This can be modeled as follows:

The addition of sodium borohydride to mercury contaminated water results in the formation of elemental mercury:

$$HgCl_2(aq) + 2NaBH_4(aq) + 6H_2O(l) \rightarrow Hg(l) + 7H_2(g) + 2B(OH)_3(aq) + 2NaCl(aq) \quad (1)$$

The elemental mercury combines with gold to form amalgam as per the Eq. 2.

$$Hg(l) + 3Au(s) \rightarrow Au_3Hg(s) \quad (2)$$

Detection and removal of boron

The concentrations of boron detected in the treated water collected from columns tested with 1.0 and 2.0 mg/L mercury are below 0.5 mg/L, the permissible limit set by WHO [6]. Figure 7A shows the absorption spectra of samples collected from column outlets tested with 1.0 and 2.0 mg/L mercury. Trace 'a' and 'b' are for 1.0 mg/L and 2.0 mg/L samples, respectively. These spectra do not have the absorbance of boron complex at 425 nm and it exactly matches with the blank spectrum. This is a clear indication of the absence of boron in the sample. Figure 7B shows the absorption spectra of the supernatant collected using magnesia as an adsorbent for boron removal. Trace 'a' is the absorption spectrum of the sample taken for the experiment and it shows a concentration of 3.5 mg/L. Trace 'b' is the absorption spectrum of the supernatant collected after one hour treatment with magnesia. It shows a drastic fall in concentration to 0.5 mg/L. Traces 'c-g' are collected after each one hour and they show a concentration below 0.25 mg/L. Traces 'h' and 'i' are collected after 12 and 24 hour, these also lack 425 nm absorbance and it indicates that there is no leakage of boron from the adsorbent. The inset of the figure shows the plot of absorbance versus time.

Inorganic mercury contamination in water is a crucial problem that people in the developing countries are facing. The proposed method is very effective for the complete removal of inorganic mercury from water. Hg(II) does not work with our adsorbent and has to be converted to Hg(0) before the treatment. Introduction of an additional reagent

Figure 7

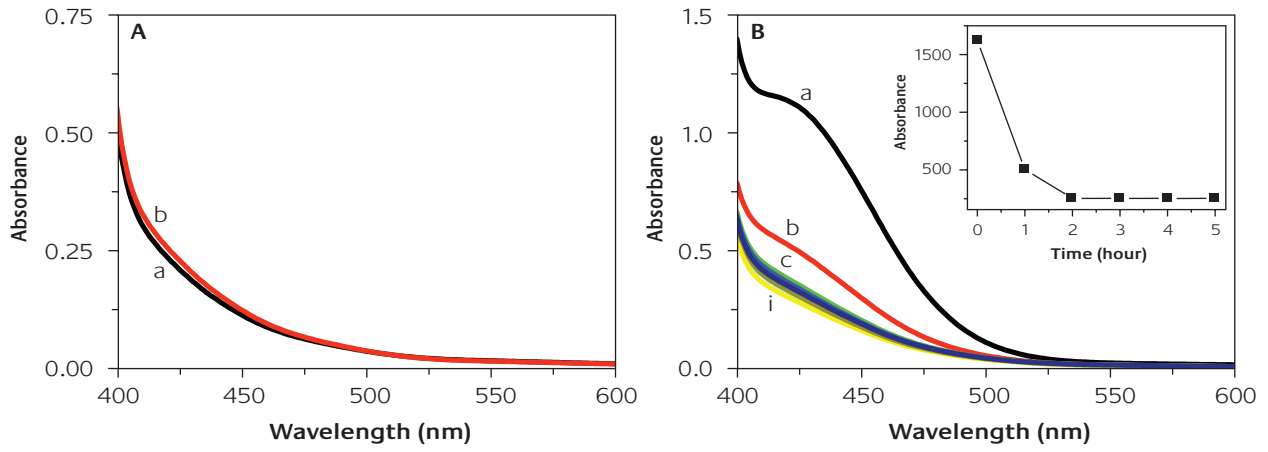

(A) UV-vis absorption spectra for the detection of boron in treated water collected from columns tested with 1.0 and 2.0 mg/L mercury concentrations. Trace 'a' is for 1.0 mg/L and trace 'b' is for 2.0 mg/L, respectively. (B)UV-vis absorption spectra of the supernatant collected from magnesia as an adsorbent. Trace 'a' is the absorption spectrum of the sample taken for the experiment. Trace 'b' is the absorption spectrum of the supernatant collected after one hour, traces 'c-g' are the spectra collected at 2, 3, 4, 5 and 6 h, respectively. Traces 'h' and 'i' are collected after 12 and 24 h, respectively. Inset is the plot of absorbance versus time

into water for the removal of a pollutant is a limitation of the study, but we have found that the concentration of boron in the treated water is below the permissible limit set by WHO and Indian standards [6, 8]. We have also studied the effectiveness of magnesia as an adsorbent for boron. We see that 3500 L of 1 mg/L mercury can be treated with 1 kg adsorbent, amount of gold required in it is only 738 mg. The cost of production of the adsorbent is low and it can be applied economically for the development of water purification systems. The expected cost for removal of 1 mg mercury is around 2.5 cents (major cost component is the cost of gold salt), which can be significantly brought down through careful gold recycling. The adsorbed mercury is mainly in the form of amalgam, and thus it is stable. The gold used can be recovered efficiently and the mercury can be disposed off without recontamination.

Conclusions

Gold nanoparticle supported on alumina is an excellent system for the removal of Hg(0) from water. Adsorption capacity was studied using a column experiment and was monitored using UV-vis spectroscopy. The time dependent removal was also studied. TEM and SEM analyses were used for understanding the morphology of the Au-Hg system. EDAX analysis and XRD confirmed the Au-Hg alloy formation. It was confirmed by control experiments that pure alumina alone is unable to remove mercury from water. Experiments revealed that the concentration of boron in the treated water is below the maximum permissible limit set by the WHO. The chemistry of metal-alloying presents a novel approach for sequestration of heavy metals. While we have studied the removal of mercury from drinking water, this study can be extended to the extraction of mercury from other sources such as industrial waste water.

Acknowledgements

World Gold Council is thanked for Project funding. The Nanoscience and Nanotechnology Initiative of the Department of Science and Technology, Government of India is thanked for equipment support.

About the authors

T. Pradeep is a professor of chemistry at the Indian Institute of Technology Madras, India. His research interests are in nanomaterials and molecular surfaces.

K.P. Lisha is currently a project fellow at the DST Unit on Nanoscience (DST UNS), Indian Institute of Technology Madras, India. Her research interests are designing of new materials for water purification.

Anshup is currently working as a project fellow with Professor Pradeep at the DST Unit on Nanoscience (DST UNS), Indian Institute of Technology Madras, India. His research interests are studies of novel nanomaterials based routes for drinking water purification and development of a low-cost integrated water purification product.

References

1 W.H. Schroeder, J. Munthes, *Atmos. Environ.*, 1998, **32**, 809
2 C.J. Lin, S.O. Pehkonen, *Atmos. Environ.*, 1999, **33**, 2067
3 F. Zahir, S.J. Rizwi, S.K. Haq, R.H. Khan, *Environ. Toxicol. Phar.*, 2005, **20**, 351
4 S. Ekino, M. Susa, T. Ninomiya, K. Imamura, T. Kitamura, *J. Neurol. Sci.*, 2007, **262**, 131
5 Study Group of Minamata Disease. Minamata Disease. Kumamoto: Kumamoto University, 1968
6 W.H.O., Guidelines for Drinking Water Quality, 3rd ed., 2004, Volume **1**
7 USEPA, Mercury Study Report to Congress, December 1997, EPA-452/R-97-003
8 Dr. R.C. Srivastava, Guidance and Awareness Raising Materials under new UNEP Mercury Programs (Indian Scenario), 2004, Centre for Environmental Pollution Monitoring and Mitigation, India
9 http://wbphed.gov.in, as accessed on 19th July 2008
10 H.G. Park, T.W. Kim, M.Y. Chae, I.K. Yoo, *Process Biochem.*, 2007, **42**, 1371
11 V. Smuleaca, D.A. Butterfield, S.K. Sikdar, R.S. Varma, D. Bhattacharyya, *J. Membrane Sci.*, 2005, **251**, 169
12 S.M. Evangelista, E.D. Oliveira, G.R. Castro, L.F. Zara, A.G.S. Prado, *Surf. Sci.*,2007, **601**, 2194
13 O. Olkhovyk, M. Jaroniec, *Adsorption*, 2005, **11**, 205
14 M.E. Mahmoud, G.A. Gohar, *Talanta*, 2000, **51**, 77
15 C.B. Lopes, M. Otero, J. Coimbra, E. Pereira, J. Rocha, Z. Lin, A. Duarte, *Micropor. Mesopor. Mat.*, 2007, **103**, 325
16 A. Oehmen, R. Viegas, S. Velizarov, M.A.M. Reis, J.G. Crespo, *Desalination*, 2006, **199**, 405
17 A. Chojnacki, K. Chojnacka, J. Hoffmann, H.Gorecki, *Miner. Eng.*, 2004, **17**, 933
18 P. Huttenloch, K.E. Roehl, K. Czurda, *Environ. Sci. Technol.*, 2003, **37**, 4269
19 H. Biester, P. Schuhmacher, G. Mueller, *Water. Res.*, 2000, **34**, 2031
20 J. Kostal, A. Mulchandani, K.E. Gropp, W. Chen, *Environ. Sci. Technol.*, 2003, **37**, 4457
21 N. Savage, M.S. Diallo, *J. Nanopart. Res.*, 2005, **7**, 331
22 M.S. Diallo, N. Savage, *J. Nanopart. Res.*, 2005, **7**, 325
23 A.S. Nair, R.T. Tom, T. Pradeep, *J. Environ. Monit.*, 2003, **5**, 363
24 A.S. Nair, T. Pradeep, *J. Nanosci. Nanotechno.*, 2007, **7**, 1
25 A.S. Nair, T. Pradeep, *Curr. Sci.*, 2003, **84**, 1560
26 Y. Chen, J. Qiu, X. Wang, J. Xiu, *J. Catal.*, 2006, **242**, 227
27 G. Riahi, D. Guillemot, M.P. Thfoin, A.A. Khodadadi, J. Fraissard, *Catal. Today*, 2002, **72**, 115
28 M.R. Regan, I.A. Banerjee, *Scripta Mater.*, 2006, **54**, 909
29 Y. Mizukoshi, T. Fujimoto, Y. Nagata, R. Oshima, Y. Maeda, *J. Phys. Chem. B*, 2000, **104**, 6028
30 M.O. Nutt, J.B. Hughes, M.S. Wong, *Environ. Sci. Technol.*, 2005, **39**, 1346
31 A. Orlov, D.A. Jefferson, N. Macleod R.M. Lambert, *Catal. Lett.*, 2004, **92**, 41
32 M. Boronat, P. Concepcion, A. Corma, S. Gonzalez, F. Illas, P. Serna, *J. Am. Chem. Soc.*, 2007, **129**, 16230
33 S. Pacheco, M. Medina, F. Valencia, J. Tapia, *J. Environ. Eng. ASCE*, 2006, **132**, 342
34 W. Yantasee, C.L. Warner, T. Sangvanich, R.S. Addleman, T.G. Carter, R.J. Wiacek, G.E. Fryxell, C. Timchalk, M.G. Warner, *Environ. Sci. Technol.*, 2007, **41**, 5114
35 M. Mullett, J. Tardio, S. Bhargava, C. Dobbs, *J. Hazard. Mater.*, 2007, **144**, 274.
36 J. Turkevich, P.L. Stevenson, J. Hillier, *Discuss Faraday Soc.*, 1951, **11**, 55
37 T.V. Ramakrishna, G. Aravamudan, M. Vijayakumar, *Anal. Chim. Acta*, 1976, **84**, 369
38 F.J. Lopez, E. Gimenez, F. Hernandez, *Fresen. J. Anal. Chem.*, 1993, **346**, 984
39 M.M.F.G. Soto, E.M. Camacho, *Sep. Purif. Technol.*, 2006, **48**, 36
40 A. Henglein, M. Giersig, *J. Phys. Chem. B*, 2000, **104**, 5056
41 JCPDS Data File No. [04-0784]
42 JCPDS Data File No. [04-0808]
43 JCPDS Data File No. [89-3711]